Heterogeneous Collapse

DOI: 10.1002/anie.201001469

EPR Spectroscopic Characterization of Local Nanoscopic Heterogeneities during the Thermal Collapse of Thermoresponsive Dendronized Polymers**

Matthias J. N. Junk, Wen Li, A. Dieter Schlüter, Gerhard Wegner, Hans W. Spiess, Afang Zhang, and Dariush Hinderberger**

Thermoresponsive polymeric materials are of great interest owing to their potential use in fields such as actuation, drug delivery, and surface modification.[1] Ever since the discovery by Wu and co-workers of the coil–globule transition of single poly(*N*-isopropylacrylamide) (PNiPAAm) chains near the lower critical solution temperature (LCST),[2] the collapse mechanism including the formation of stable mesoglobules have been intense topics of research.[1,3] Despite these efforts, a molecular-scale picture of what happens when thermoresponsive polymers start to dehydrate at a certain temperature, subsequently collapse, and then assemble to mesoglobules, does not exist. This absence severely hampers rational materials design.

In an exploratory research effort aimed at detecting unusual properties of dendronized polymers,[4] we recently discovered that such systems based on oligoethyleneglycol (OEG) units exhibit fast and fully reversible phase transitions with a sharpness that is amongst the most extreme ever observed.[5] These dendronized polymers with terminal ethoxy groups are soluble in water and their lower critical solution temperature (LCST) is found in a physiologically interesting temperature regime between 30 and 36 °C. The LCST of these OEG dendronized polymers is as low as for poly(ethylene oxide) and long-chain ethylene oxide oligomers. For the latter, the influence of hydrophobic end groups on the LCST has been thoroughly investigated, both experimentally and theoretically.[6] Given this extraordinary behavior, these polymers should be particularly suited to gaining a deeper understanding of the processes involved. Such materials also bear great potential as hosts for small molecules for targeted release, as they have encapsulation properties, which can be controlled by thermoresponsivity.[7]

There are indications that such thermal responses proceed by the formation of structural inhomogeneities of variable lifetimes on the nanometer scale that are still poorly understood. Indeed, this topic has been identified as one of the major challenges of research in the macromolecular sciences in the coming years.[8] Herein, the focus is on a clearer understanding of the formation, structure, and lifetimes of these local inhomogeneities, the effect of the individual chemical structures on the physical processes, and the influence of the local heterogeneities on the aspired function (for example, drug delivery).

The remarkable macroscopic behavior of such materials results from the systems being far from classical macroscopic equilibrium. This situation can be viewed as an example of "molecularly controlled non-equilibrium". Such macromolecule-based processes far from equilibrium are extensively found in nature, for example in DNA replication, to obtain high specificity in the noisy environment of a cell. Investigations into similar concepts in synthetic macromolecular systems are still rare.[9,10]

Magnetic resonance techniques as intrinsically local methods meet the conditions required to solve questions involved with structural inhomogeneities of functional macromolecules[11] and dynamic heterogeneities in polymer melts in the vicinity of the glass transition.[12] Advanced NMR and pulse EPR techniques have now been established for the study of biological and synthetic macromolecules.[10–15] A particularly simple way of studying the molecular environment of systems undergoing a thermal transition utilizes conventional continuous wave (CW) EPR spectroscopy on nitroxide radicals as paramagnetic tracer molecules. Such spin probes are sensitive to the local viscosity, which gives rise to changes in the rotational correlation time, and to the local polarity/hydrophilicity.[11c,14,15] The polarity affects the electronic structure of the radical and changes the spectral parameters, specifically the *g* factor and the hyperfine coupling constant to ^{14}N. The amphiphilic radical 2,2,6,6-tetramethylpiperidine-1-oxyl (TEMPO) is especially suited to sample both hydrophobic and hydrophilic regions. It has been successfully applied to observe structural nanoinhomogeneities formed in thermoresponsive poly(*N*-isopropylacrylamide)-based hydrogels upon thermally induced macrosopic

[*] M. J. N. Junk,[+] Prof. Dr. G. Wegner, Prof. Dr. H. W. Spiess, Dr. D. Hinderberger
Max-Planck-Institut für Polymerforschung
Ackermannweg 10, 55128 Mainz (Germany)
Fax: (+49) 6131-379-100
Dr. W. Li,[+] Prof. Dr. A. D. Schlüter, Prof. Dr. A. Zhang[#]
Institut für Polymere, Department of Materials, ETH Zurich
Wolfgang-Pauli-Straße 10, HCI G525, 8093 Zürich (Switzerland)
Fax: (+41) 44-6331390
E-mail: azhang@shu.edu.cn
[#] Current address: Department of Polymer Materials
Shanghai University, Chengzhong Street 20
Shanghai 201800 (China)
[+] These authors contributed equally to this work.

[**] We thank Christian Bauer and Susan Pinnells for technical support. M.J.N.J. gratefully acknowledges financial support from the Fonds der chemischen Industrie (FCI) and from the Graduate School of Excellence "Materials Science in Mainz" (MAINZ).

Supporting information for this article is available on the WWW under http://dx.doi.org/10.1002/anie.201001469.

collapse. These nanoinhomogeneities were static over a timescale of at least two hours.[15] Based on previous experience and tests with TEMPO and the more hydrophilic TEMPOL (see Supporting Information), TEMPO was identified as the spin probe of choice. Thus, CW EPR spectroscopy on TEMPO was applied to aqueous solutions of the dendronized polymers, thus allowing insights to be gained into the molecular processes associated with the thermal transition.

Representative CW EPR spectra of TEMPO in an aqueous solution of 10 wt% PG1(ET) (Scheme 1) well above and below the critical temperature (T_C) of 33 °C are shown in Figure 1a. Whilst the low-field and center peaks remain almost unaffected, the high-field line, which is most sensitive to structural and dynamic effects, changes considerably, and it is shown in Figure 1b at various temperatures. The apparent splitting of this line at elevated temperatures originates from two nitroxide species **D1** and **D2** that are placed in local environments with different polarities. This gives rise to considerable differences of the isotropic hyperfine coupling constants a_{iso} (and the g values g_{iso}).

Before proceeding further, we checked whether the critical temperatures from turbidity measurements and EPR spectroscopy coincided. The polymers in this study are polymethacrylate derivatives with first-, second-, and third-generation triethyleneoxide dendrons (PG1—3(ET); Scheme 1). Furthermore, a second-generation dendronized polymethacrylate was investigated in which the triethyleneoxide core was replaced by a hydrophobic octane unit (PG2(ETalkyl); Scheme 1). The turbidity measurements reflect a phase separation process of a seemingly classical nature, in which droplets of a concentrated solution of the polymer separate from the dilute solution of the polymer (binodal decomposition). The droplets of the concentrated phase were identified by light microscopy.[5a] The EPR-derived T_C values were found from plots of the spectral fraction of nitroxide species **D1** as a function of temperature; T_C is defined as the temperature at which a virtually constant spectral fraction of nitroxide species **D1** starts to decrease markedly (Supporting Information, Figure S3). Indeed, the critical temperatures determined for PG1(ET) (T_C from EPR: 32 °C, from turbidity: 33 °C), PG2(ET) (34 °C, 36 °C), PG3(ET) (34 °C, 34 °C), and PG2(ETalkyl) (30 °C, 31 °C) are almost identical, regardless of whether they were obtained from EPR or turbidity measurements. The slightly lower EPR-derived values are due to higher concentrations of the polymer solutions. The macroscopic phase separation identified by turbidimetry is due to the fact that water becomes a thermodynamically poor solvent for the oxyethylene segments as the temperature increases. The gel phase formed in equilibrium with the dilute phase is however still highly swollen by water. The objective of our studies presented

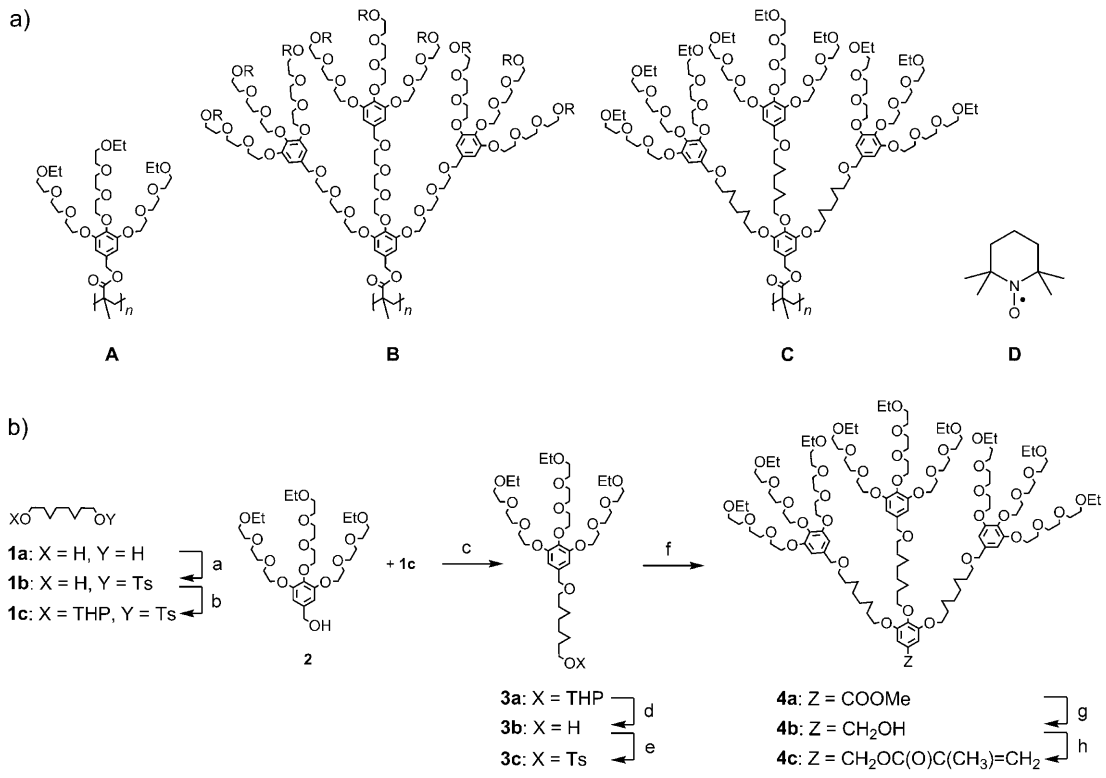

Scheme 1. a) Thermoresponsive dendronized polymers PG1(ET) (**A**), PG2(ET) (**B**, R = Et), PG3(ET) (**B**, R = $(H(CH_2CH_2O)_4)_3Ph$), PG2(ETalkyl) (**C**), and the spin probe TEMPO (**D**). b) Synthetic route to the PG2(ETalkyl) monomer. Reagents and conditions: a) NaOH, TsCl, THF, H_2O, 0–25 °C, 3 h (56%); b) DHP, PPTS, −5–25 °C, 4.5 h (86%); c) KI, [15]crown-5, NaH, THF, RT, 12 h (96%); d) PTSA, MeOH, RT, 2 h (90%); e) TsCl, TEA, DMAP, DCM, −5–25 °C, 3 h (89%); f) methyl gallate, K_2CO_3, KI, DMF, 80 °C, 24 h (83%); g) LAH, THF, −5 °C–25 °C, 2.5 h (95%); h) MAC, DMAP, TEA, DCM, −5–25 °C, 3 h (84%). DHP = 3,4-dihydro-2*H*-pyran, PPTS = pyridinium toluenesulfonate; PTSA = *p*-toluenesulfonic acid; LAH = lithium aluminum hydride; MAC = methacryloyl chloride; DMAP = *N*,*N*-dimethylaminopyridine; TEA = triethylamine.

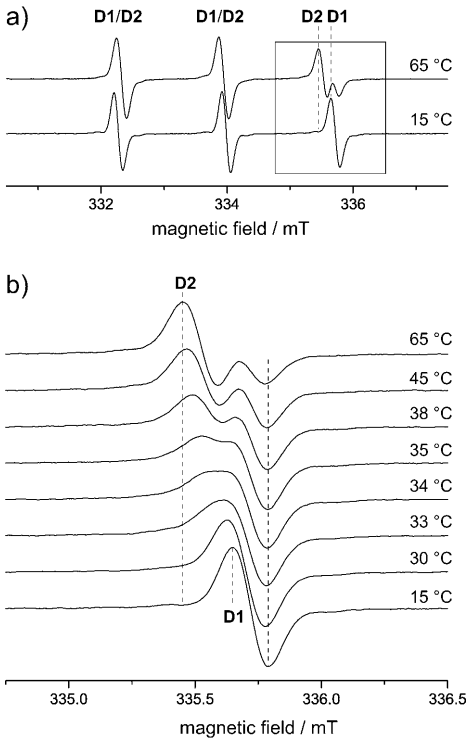

Figure 1. a) CW EPR spectra (X-band, microwave frequency ca. 9.3 GHz) for 0.2 mM TEMPO in an aqueous solution of 10 wt% PG1(ET) recorded at 15 °C and 65 °C. b) Detailed plot of the high-field transition line ($m_I = -1$, marked by a rectangle in (a)) at selected temperatures. The contribution to the high field peak at 335.4 mT, denoted **D2**, originates from TEMPO molecules in a hydrophobic environment, whilst nitroxides in a hydrophilic surrounding give rise to the contribution **D1** at 335.65 mT. The broken lines at the outer extrema of the peak serve as guides to the eye.

below was to analyze the properties of this gel phase as seen by the spin probe.

The spectroscopic parameters for component **D1** coincide with those of TEMPO in pure water ($a_{\mathbf{D1}} \approx 48.3$ MHz); that is, this spin probe is located in a strongly hydrated, hydrophilic environment. The observed decrease of a_{iso} by 3.7 MHz for species **D2** at 65 °C is indicative of much more hydrophobic and less hydrated surroundings for these spin probes (comparable to chloroform or *tert*-butanol).[16] At temperatures below T_C, only the hydrophilic component **D1** is observed as all dendritic units are water-swollen. Above the critical temperature of 33 °C, an increasing fraction of hydrophobic species **D2** is observed with increasing temperature. The dehydration of the dendritic units thus leads to a local phase separation with the formation of hydrophobic cavities.

More strikingly, the peak position of the component **D2** is not fixed, but approaches its final value only at temperatures well above T_C. This indicates a dynamic exchange of the spin probes between hydrophilic and hydrophobic regions. This exchange leads to an intermediate hyperfine coupling constant that is an effective weighted average between the two extreme values of the hydrophilic and the (static) hydrophobic regions at 65 °C. Thus, the inhomogeneities formed upon the phase separation are not static but dynamic, and they strongly influence the EPR spectral shape.

The exchange detected by the spin probes can be caused by two effects: hopping of the spin probe between collapsed and hydrated polymer aggregate regions, or fluctuations of the aggregates themselves. The latter can be viewed as a fast opening and closing of hydrophobic cavities or a fast swelling and de-swelling of regions surrounding the spin probe. The size of the inhomogeneities can be estimated by the translational displacement of TEMPO in the polymer matrix, given by $\langle x^2 \rangle = 6 D_T \tau_T$. At $T = 34$ °C, a maximum translational displacement $\langle x^2 \rangle^{1/2} \leq 5.1$ nm of the spin probes due to diffusion is obtained; this diffusion is assisted by fluctuations of the polymer undergoing the thermal transition (for details, see the Supporting Information).[17,18] Thus we can conclude that slightly above T_C, the few hydrophobic cavities formed are still small, that is, in the range of a few nanometers. Spin probe movement and/or local polymer fluctuations then lead to an exchange of the probe molecules on the EPR timescale between the hydrophobic and large hydrophilic regions. The hydrophilic regions are still overwhelmingly more abundant and the fraction of species **D1** in these regions is larger than 60 % (see Figure 2b). The spin probes thus mainly sample the interface between the two fundamentally different regions. Note that a few local dynamic heterogeneities on a nanometer scale are sufficient to induce a macroscopically observable (by turbidity measurements) transition in the sample. Remarkably, the transition is detected at the same temperature by two methods probing length scales which differ by at least two orders of magnitude. This suggests that the small hydrophobic regions detected by EPR might be visualized as cross-links affecting the organization of the dendronized macromolecules on much larger scales. The sharp macroscopic transition can then be viewed as the onset of a complex de-swelling process that is broad rather than a sharp transition on the molecular scale. The existence of clusters in oligoethylene oxides as a function of temperature and concentration has long been observed, and has been attributed to the oxyethylene segments becoming increasingly hydrophobic with increasing temperature.[19]

An increase in temperature leads not only to an increase in the fraction of the hydrophobic regions, but also their size grows, and exchange of probe molecules between hydrophobic and hydrophilic sites becomes unlikely. The spin probes now sample the bulk hydrophobic (and remaining hydrophilic) regions rather than their interface. Together with the increase in size, the dynamics of the polymer fluctuations slow down, as both effects are coupled. In combination, a final state of distinct hydrophobic and hydrophilic regions is observed that are static on the EPR timescale.

To quantify aggregation and collapse associated with the thermally induced transition, effective hyperfine coupling constants of those TEMPO molecules in hydrophobic environments $a_{\mathbf{D2}}$ and the fraction of TEMPO in hydrophilic environments $y_{\mathbf{D1}}$ were determined as a function of temperature. EPR lineshapes were fitted to these parameters (see the Experimental Section in the Supporting Information).[20] By plotting these parameters against the reduced temperature $(T - T_C)/T_C$ it is then possible to check whether the collapse results from a well-behaved phase transition. As can be seen in Figure 2, both parameters do not follow one straight line, as

expected for a simple phase transition, but instead strongly deviate from linearity.[21] Figure 2a shows that static, non-exchanging hyperfine coupling values a_{D2} are not reached until around 30 °C above the critical temperature. Thus, in this wide temperature range, a complex dehydration takes place that cannot be described as a classical phase transition based on a single de-swelling process. For all the polymers, at least two dehydration processes are found, as indicated by the different straight lines. The first process takes place at temperatures slightly above the critical temperature ($(T-T_C)/T_C < 0.02$), the second process in a temperature regime far above T_C. Extrapolations of the two linear fits meet at around $(T-T_C)/T_C = 0.02$ (ca. 7 °C above T_C) for all the polymers, thus indicating that in all cases the collapse processes are equivalent. These results suggest that in this narrow temperature range, the major part of the dehydration takes place, as a_{D2} in this interval is reduced to values already close to the static final values. A further increase in temperature results in only smaller changes of a_{D2}, which is a sign of the expulsion of smaller amounts of residual water from the collapsed polymeric regions.

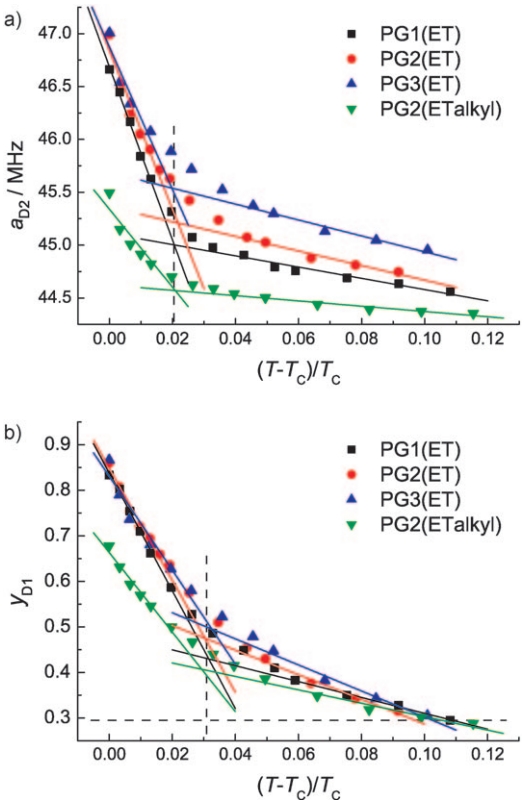

Figure 2. a) The hyperfine splitting constant of the hydrophobic spectral component a_{D2} as a function of the reduced temperature $T_r = (T-T_C)/T_C$ for 0.2 mM TEMPO in 10 wt% aqueous solutions of four dendronized polymers, which differ in the dendron generation (PG1(ET), PG2(ET), and PG3(ET)) and the structural properties of the dendritic core (PG2(ETalkyl)). b) Variation of the fraction of TEMPO in a hydrophilic environment y_{D1} with increasing temperature for the above-specified polymers. Two linear fits of data points close to and far from the critical temperature illustrate at least two different de-swelling processes, clearly indicating that the temperature-induced collapse of the polymers under investigation cannot be described by a thermodynamic phase transition. The reduced temperature at which the two lines meet, which is common to all the polymers under investigation, is indicated by a dashed line.

Straight-line best fits to two processes are obtained for those polymers with no or a hydrophobic dendritic core (PG1(ET) and PG2(ETalkyl)). For those materials possessing a hydrophilic dendritic core (PG2(ET) and PG3(ET)), a significant deviation from the simple two-process fit is observed, indicating that the collapse is not fully described by two well-defined processes. Moreover, the first process turns out to be most effective when the dehydration is supported by a hydrophobic core, as in the case of PG2-(ETalkyl). It deteriorates when the core contains oxyethylene groups, which can trap more water.

Qualitatively, the same behavior is seen in Figure 2b for the temperature-dependent fraction of TEMPO in a hydrophilic environment y_{D1}. The same intersection point of the two linear fits is found, and the dependence of the efficiency of the first strong dehydration process on the chemical structure described in Figure 2a is again manifest in Figure 2b. However, the graphs show one major difference: At high temperatures, y_{D1} is only determined by the volume fraction of the collapsed polymer in water and thus approaches 0.3 for all polymer solutions. In contrast, the (static) isotropic hyperfine values of TEMPO in hydrophobic regions a_{D2} differ depending on the structure of the dendronized polymer. PG2-(ETalkyl), which has a hydrophobic core, provides the most hydrophobic environment, followed by PG1(ET) bearing no core, and PG2(ET) with a hydrophilic ethyleneoxide core; the least hydrophobic regions are provided by PG3(ET) bearing an extended hydrophilic core. The differences can be explained by the hydrophilic cores entrapping more residual water molecules. This effectively increases the hydrophilicity of the environment of the entrapped spin probe.

The data in Figure 2 support the picture of a few small hydrophobic patches triggering a macroscopically observable transition to a gel phase that is still highly swollen by water and is composed of regions differing in local water concentration. Furthermore, the process in the first temperature interval is in agreement with a growing number of uncorrelated hydrophobic regions up to a concentration and/or a volume fraction that is similar to that of the remaining hydrophilic regions (thus the kink at $y_{D1} \approx 0.5$). This could be an indication that the growth of hydrophobic regions reaches a threshold that could be interpreted as a percolation point. When the fractions of species **D1** to **D2** become equal, the likelihood of two hydrophobic regions (which up to that point can be largely uncorrelated) becoming neighbors increases immensely and the role of the interface becomes less important.[22]

In conclusion, the collapse transition of thermoresponsive dendronized polymers with different cores was characterized on a molecular scale by CW EPR spectroscopy. When the temperature is raised above T_C, the aggregation of the complete polymer sample is triggered by dynamic structural inhomogeneities of a few nanometers: The employed spin probes in this temperature regime exchange between large hydrophilic and small hydrophobic regions. Whilst macroscopic turbidity measurements suggest a sharp phase tran-

sition of the polymer, this study reveals that the dehydration of the polymer chains proceeds over a temperature interval of at least 30 °C. It cannot be described by a single de-swelling process that would be expected for a thermodynamic phase transition. Rather, the dehydration should be viewed as a molecularly controlled non-equilibrium state and takes place in two steps. Within about 7 °C above T_C, the majority of the dehydration is completed and percolation for the fraction and volume of hydrophobic regions is reached. Heating the samples even higher only leads to an additional loss of residual water from the collapsed system. While the aggregation temperature mainly depends on the periphery of the dendrons, the dehydration efficiency is strongly related to the hydrophobicity of the core.

Received: March 11, 2010
Revised: April 13, 2010
Published online: July 2, 2010

Keywords: EPR spectroscopy · nanostructures · non-equilibrium processes · phase transitions · polymers

[1] a) H. G. Schild, *Prog. Polym. Sci.* **1992**, *17*, 163 – 249; b) C. de Las Heras Alarcón, S. Pennadam, C. Alexander, *Chem. Soc. Rev.* **2005**, *34*, 276 – 285; c) R. Yerushalmi, A. Scherz, M. E. van der Boom, H.-B. Kraatz, *J. Mater. Chem.* **2005**, *15*, 4480 – 4487; d) Z. Jia, H. Chen, X. Zhu, D. Yan, *J. Am. Chem. Soc.* **2006**, *128*, 8144 – 8145; e) A. Kumar, A. Srivastava, I. Y. Galaev, B. Mattiasson, *Prog. Polym. Sci.* **2007**, *32*, 1205 – 1237; f) H. Chen, Z. Jia, D. Yan, X. Zhu, *Macromol. Chem. Phys.* **2007**, *208*, 1637 – 1645.

[2] a) C. Wu, S. Q. Zhou, *Macromolecules* **1995**, *28*, 5388 – 5390; b) C. Wu, S. Q. Zhou, *Macromolecules* **1995**, *28*, 8381 – 8387; c) C. Wu, S. Q. Zhou, *Phys. Rev. Lett.* **1996**, *77*, 3053 – 3055; d) X. Wang, X. Qiu, C. Wu, *Macromolecules* **1998**, *31*, 2972 – 2976.

[3] For example see: a) K. Van Durme, S. Verbrugghe, F. E. Du Prez, B. Van Mele, *Macromolecules* **2004**, *37*, 1054 – 1061; b) S. Luo, J. Xu, Z. Zhu, C. Wu, S. Liu, *J. Phys. Chem. B* **2006**, *110*, 9132 – 9138; c) Y. Ono, T. Shikata, *J. Am. Chem. Soc.* **2006**, *128*, 10030 – 10031; d) H. Cheng, L. Shen, C. Wu, *Macromolecules* **2006**, *39*, 2325 – 2329; e) K. Van Durme, G. Van Assche, V. Aseyev, J. Raula, H. Tenhu, B. Van Mele, *Macromolecules* **2007**, *40*, 3765 – 3772; f) Y. Ono, T. Shikata, *J. Phys. Chem. B* **2007**, *111*, 1511 – 1513; g) M. Keerl, V. Smirnovas, R. Winter, W. Richtering, *Angew. Chem.* **2008**, *120*, 344 – 347; *Angew. Chem. Int. Ed.* **2008**, *47*, 338 – 341; h) M. Keerl, J. S. Pedersen, W. Richtering, J. Am. Chem. Soc. 2009, 131, 3093 – 3097.

[4] a) A. D. Schlüter, J. P. Rabe, *Angew. Chem.* **2000**, *112*, 860 – 880; *Angew. Chem. Int. Ed.* **2000**, *39*, 864 – 883; b) A. Zhang, L. Shu, Z. Bo, A. D. Schlüter, *Macromol. Chem. Phys.* **2003**, *204*, 328 – 339; c) A. D. Schlüter, *Top. Curr. Chem.* **2005**, *245*, 151 – 191; d) H. Frauenrath, *Prog. Polym. Sci.* **2005**, *30*, 325 – 384. See also: e) B. M. Rosen, C. J. Wilson, D. A. Wilson, M. Peterca, M. R. Imam, V. Percec, *Chem. Rev.* **2009**, *109*, 6275 – 6540.

[5] a) W. Li, A. Zhang, K. Feldman, P. Walde, A. D. Schlüter, *Macromolecules* **2008**, *41*, 3659 – 3667; b) W. Li, A. Zhang, A. D. Schlüter, *Chem. Commun.* **2008**, 5523 – 5525; c) W. Li, D. Wu, A. D. Schlüter, A. Zhang, *J. Polym. Sci. Part A* **2009**, *47*, 6630 – 6640.

[6] E. E. Dormidontova, *Macromolecules* **2004**, *37*, 7747 – 7761.

[7] B. Helms, J. M. J. Frechet, *Adv. Synth. Catal.* **2006**, *348*, 1125 – 1148.

[8] C. K. Ober, S. Z. D. Cheng, P. T. Hammond, M. Muthukumar, E. Reichmanis, K. L. Wooley, T. P. Lodge, *Macromolecules* **2009**, *42*, 465 – 471.

[9] a) F. Cady, H. Qian, *Phys. Biol.* **2009**, *6*, 036011; b) D. Brutlag, A. Kornberg, *J. Biol. Chem.* **1972**, *247*, 241 – 248.

[10] G. P. Drobny, J. R. Long, T. Karlsson, W. Shaw, J. Popham, N. Oyler, P. Bower, J. Stringer, D. Gregory, M. Mehta, P. S. Stayton, *Annu. Rev. Phys. Chem.* **2003**, *54*, 531 – 571.

[11] a) K. Schmidt-Rohr, H. W. Spiess, *Multidimensional Solid-State NMR and Polymers*, Academic Press, London, **1994**; b) K. Saalwächter, *Prog. Nucl. Magn. Reson. Spectrosc.* **2007**, *51*, 1 – 35; c) S. Schlick, *Advanced ESR Methods in Polymer Research*, Wiley-Interscience, Hoboken, **2006**.

[12] a) K. Schmidt-Rohr, H. W. Spiess, *Phys. Rev. Lett.* **1991**, *66*, 3020 – 3023; b) A. Heuer, M. Wilhelm, H. Zimmermann, H. W. Spiess, *Phys. Rev. Lett.* **1995**, *75*, 2851 – 2854; c) U. Tracht, M. Wilhelm, A. Heuer, H. Feng, K. Schmidt-Rohr, H. W. Spiess, *Phys. Rev. Lett.* **1998**, *81*, 2727 – 2730.

[13] a) M. R. Hansen, T. Schnitzler, W. Pisula, R. Graf, K. Müllen, H. W. Spiess, *Angew. Chem.* **2009**, *121*, 4691 – 4695; *Angew. Chem. Int. Ed.* **2009**, *48*, 4621 – 4624; b) S. Ruthstein, A. M. Raitsimring, R. Bitton, V. Frydman, A. Godt, D. Goldfarb, *Phys. Chem. Chem. Phys.* **2009**, *11*, 148 – 160; c) D. Hinderberger, H. W. Spiess, G. Jeschke, *Appl. Magn. Reson.* **2010**, *37*, 657 – 683; d) C. Dockter, A. Volkov, C. Bauer, Y. Polyhach, Z. Joly-Lopez, G. Jeschke, H. Paulsen, *Proc. Natl. Acad. Sci. USA* **2009**, *106*, 18485 – 18490.

[14] a) D. Hinderberger, O. Schmelz, M. Rehahn, G. Jeschke, *Angew. Chem.* **2004**, *116*, 4716 – 4721; *Angew. Chem. Int. Ed.* **2004**, *43*, 4616 – 4621; b) R. Owenius, M. Engstrom, M. Lindgren, M. Huber, *J. Phys. Chem. A* **2001**, *105*, 10967 – 10977.

[15] M. J. N. Junk, U. Jonas, D. Hinderberger, *Small* **2008**, *4*, 1485 – 1493.

[16] B. R. Knauer, J. J. Napier, *J. Am. Chem. Soc.* **1976**, *98*, 4395 – 4400.

[17] A. L. Kovarskii, A. M. Wasserman, A. L. Buchachenko, *J. Magn. Reson.* **1972**, *7*, 225 – 237.

[18] N. M. Atherton, *Principles of Electron Spin Resonance*, Ellis Horwood, New York, **1993**.

[19] N. Derkaoui, S. Said, Y. Grohens, R. Olier, M. Privat, *J. Colloid Interface Sci.* **2007**, *305*, 330 – 338.

[20] S. Stoll, A. Schweiger, *J. Magn. Reson.* **2006**, *178*, 42 – 55.

[21] P. M. Chaikin, T. C. Lubensky, *Principles of Condensed Matter Physics*, Cambridge University Press, **1995**.

[22] Note that at the chosen polymer and spin probe concentrations, about 30 % of the spin probes reside in hydrophilic regions even at high temperatures. Therefore, the proposed percolation point at $y_{D1} \approx 0.5$ appears when $(0.5/0.7 \approx 0.7)$ 70 % of all probes taking part in the transition are trapped in hydrophobic regions.

